OTX2 signals from the choroid plexus to regulate adult neurogenesis

Anabelle Planques[1], Vanessa Oliveira Moreira[1], Chantal Dubreuil, Alain Prochiantz, Ariel A Di Nardo[*]

Centre for Interdisciplinary Research in Biology (CIRB), Collège de France, CNRS UMR 7241, INSERM U1050, PSL Research University, Paris, France.

[1]co-first authors
[*]corresponding author: ariel.dinardo@college-de-france.fr

Abstract
Proliferation and migration during adult neurogenesis are regulated by a microenvironment of signaling molecules originating from local vasculature, from cerebrospinal fluid produced by the choroid plexus, and from local supporting cells including astrocytes. Here, we focus on the function of OTX2 homeoprotein transcription factor in the mouse adult ventricular-subventricular zone (V-SVZ) which generates olfactory bulb neurons. We find that OTX2 secreted by choroid plexus is transferred to supporting cells of the V-SVZ and rostral migratory stream. Deletion of *Otx2* in choroid plexus reduces the number of olfactory bulb newborn neurons and modifies extracellular matrix components produced by astrocytes. Similar results are obtained by expressing secreted single-chain antibodies to sequester OTX2 in the cerebrospinal fluid, demonstrating the importance of non-cell autonomous OTX2 in adult neurogenesis and suggesting a pivotal role for astrocytes. Thus, we reveal a multi-level and non-cell autonomous role of a homeoprotein and reinforce the choroid plexus as a key niche compartment affecting adult neurogenesis.

Introduction

Neurogenesis in the adult mouse brain provides continuous replacement of interneurons in olfactory bulbs (OB) and is important for olfaction-based learning (Lledo and Valley, 2016). Neural stem cells (NSCs), located in the adult ventricular-subventricular zone (V-SVZ) lining the lateral cerebral ventricles, give rise to progenitor cells (first transient amplifying cells that generate migrating neuroblasts) that migrate though the rostral migratory stream (RMS) to reach the OB where they differentiate as interneurons and integrate into local circuitry. This process is regulated not only by factors intrinsic to the NSCs and progenitors but also by their microenvironment consisting of factors from local vasculature, neuronal circuits, cerebrospinal fluid (CSF) and local supporting cells (Lehtinen et al., 2013; Silva-Vargas et al., 2013; Bjornsson et al., 2015). For example, it has been shown that NSCs contact vascular endothelial cells and project into the ventricular wall where their cilia contact CSF, which participates in regulating proliferation and migration through mechanical influence and CSF-borne factors (Sawamoto et al., 2006; Mirzadeh et al., 2008; Shen et al., 2008; Petrik et al., 2018).

The CSF is produced within brain ventricles by the choroid plexuses (ChP) which express many secreted factors found to influence neurogenesis, including growth factors, morphogens and guidance clues (Falcão et al., 2012; Kokovay et al., 2012; Silva-Vargas et al., 2016). Neuroblasts and NSCs also contact local non-neurogenic astrocytes which secrete factors that help establish and maintain the microenvironment and can influence neurogenesis (Lois et al., 1996; Shen et al., 2008; Girard et al., 2014; Gengatharan et al., 2016).

Homeoproteins are key regulators of neurogenesis both during embryogenesis and in the adult (Curto et al., 2014; Prochiantz and Di Nardo, 2015). This class of transcription factors have the property to act both cell-autonomously and non-cell-autonomously after secretion and internalization in target cells. The OTX2 homeoprotein is expressed by ChP, secreted in CSF, and transfers in brain parenchyma to regulate visual cortex plasticity in postnatal mice (Spatazza et al., 2013). OTX2 is a regulator of embryonic development and embryonic neurogenesis (Yang et al., 2014; Hoch et al., 2015; Acampora et al., 2016) but its role on adult neurogenesis has not been investigated. We show that OTX2 transfers in supporting cells and impacts neurogenesis in part by modifying the expression of astrocyte-derived extracellular factors.

Materials and Methods

Animals

S129 mice were purchased from Charles River Laboratories. The *Otx2*$^{lox/lox}$ (Otx2-lox) mice were kindly donated by Dr. T. Lamonerie (Fossat et al., 2006) and *Otx2*$^{+/GFP}$ mice were kindly donated by Dr. A. Simeone (Acampora et al., 2009). The single chain antibody (scFv) knock-in mouse model (scFv-Otx2 mice) were previously described (Bernard et al., 2016). All animal procedures, including housing, were carried out in accordance with the recommendations of the European Economic Community (86/609/EEC), the French National Committee (87/848) and French bylaws (AGRG1240332A / AGRG1238724A / AGRG1238767A / AGRG1238729A / AGRG1238753A). For surgical procedures, animals were anesthetized with Xylazine (Rompun 2%, 5 mg/kg) and Ketamine (Imalgene 500, 80 mg/kg). For biochemical analysis, mice were sacrificed by cervical elongation. This research (project no. 00704.02) was approved by Ethics committee n° 59 of the French Ministry for Research and Higher Education. Mice were conventionally raised (12:12 hours light:dark cycle) in cages with red tunnels, nesting cotton, and with food and water ad libitum.

Mouse surgery

Cre-Tat recombinant protein (8 to 20 µg/ml in 400 mM NaCl, 15% DMSO) or vehicle was injected as previously described (Spatazza et al., 2013). 10 days after Cre-Tat injection, mice were injected intraperitonally with 150 mg/kg of BrdU (Sigma B9285 at 10 mg/ml diluted in NaCl 0.9%). For OB integration experiments, mice were injected with BrdU twice daily for five days, and then housed for 3 weeks prior to perfusion with PBS. For proliferation experiments, mice were injected with one pulse of BrdU and then perfused with PBS two hours later. Brains were cut in half along the anterior-posterior axis: the anterior half was fixed for 48 h at 4 °C in 4% formaldehyde-PBS, immersed overnight in 20% sucrose PBS, and processed for cryostat sectioning; the posterior half was used to recover 4th ventricle ChP for quantitative PCR analysis of *Otx2* expression.

Astrocyte cell culture

Primary astrocytes were prepared from cortex of newborn mouse (P0 to P4) and cultured in 10 mL of DMEM high glucose, 10% serum, 1x antimitotic/antibiotic. After 7 days, astrocytes were passaged into 6-well plates at 400 000 cells/ml, incubated 14 days, and then were treated with 1% Ara-C (in DMEM high glucose, 1% B27, 1x antimitotic/antibiotic) for 24 h prior to treatment with 100 ng/ml OTX2 protein. After 24 h, treated astrocytes were processed for quantitative PCR analysis.

Immunohistochemistry and histology

Frozen brains were sectioned (25 µm) by cryostat and stored at -20 °C. Slides were thawed 15 min at room temperature, hydrated in PBS, and incubated in a steamer for 15 min with 10 mM citrate buffer, pH 6. After cooling, sections were washed with PBS and incubated in blocking buffer (0.5% Triton-X, 10% normal donkey serum (Abcam) in PBS) for 30 min. Primary antibodies were incubated overnight at room temperature (1/100 anti-BrdU OBT0030 ABD Serotech; 1/400 anti-Caspase # 9661 Cell Signaling; 1/250 anti-OTX2 ab92326 Abcam; 1/1000 anti-DCX AB2253 Millipore; 1/200 anti-GFAP G6171 Sigma; 1/1000 anti-Vimentin AB5733 Millipore; 1/1000 anti-GFP ab13970 Abcam). After PBS washes, secondary antibodies were incubated 2 h at room temperature (1/2000 donkey anti-IgG Alexa fluor Invitrogen or 1/500 anti-guinea pig biotinylated ab6907 Abcam). Sections treated with biotinylated secondary antibodies were further incubated 2 h with dye-conjugated streptavidin (Invitrogen). Sections were dried and mounted in DAPI Fluoromount-G. TUNEL was performed with the *in situ* cell death detection kit (Roche) according to manufacturer instructions. Imaging was performed

with an SP5 inverted confocal microscope (Leica), a Nikon 90i upright widefield, or a Spinning-disk confocal with constant parameters. For BrdU analysis, one section every 200 µm was quantified. Counting was performed using ImageJ software with systematic methods (background correction and thresholding). *In situ* hybridization was performed as previously described (Spatazza et al., 2013).

Quantitative PCR

Total RNA from 4th ventricle ChP was extracted with the RNeasy Lipid Tissue Mini Kit (Qiagen) with DNA removal. RNA and protein were extracted for ECM composition analysis using the AllPrep DNA/RNA/Protein Mini Kit (Qiagen). RNA was processed with the QuantiTect Reverse Transcription Kit (Qiagen). cDNA was diluted 1/10 with RNase-free water for quantitative PCR, samples, which were analyzed in triplicate with a LightCycler 480 II (Roche) and SYBR Green I Master mix. After T_m profile validation, gene-to-HPRT ratios were determined by the $2^{-\Delta\Delta Ct}$ method. For *Otx2* expression analysis, mean expression of vehicle-injected mice was used for comparison.

Microdissection

Brain was placed in cold PBS, dorsal side facing up, and two equidistant longitudinal incisions in each OB were made to divide them in 3 parts while keeping them attached to the rest of the brain. The V-SVZ microdissection was performed as previously described (Mirzadeh et al., 2010). Afterwards, the hemispheres were placed once again dorsal side facing up and the two sagittal cuts starting from the OB incisions were pursued along the entire length of the brain. The central piece of tissue was laid on its side and RMS was excised as shown in Fig. 2*D*. All tissue was stored at -80 °C.

Immunoprecipitation and Western blot

Microdissections were triturated in 100 µl of lysis buffer (150 mM NaCl, 1% Triton, 100 mM Tris, pH 7.4, 10 mM EDTA, 1X protease/phosphatase inhibitor (Roche)) per 10 mg of tissue and incubated 10 min on ice. Supernatant was recovered in low-bind tubes after centrifugation for 10 min at 16 000 *g*. Antibody was added (2.5 µg of anti-OTX2 (ab21990, Abcam) or anti-IgG (ab27478, Abcam) and incubated overnight at 4 °C with rotation. Protein A sepharose beads (GE Healthcare) were washed twice and resuspended 1:1 with lysis buffer. Beads (30 µl) were added to each sample and incubated 3 h at 4 °C. Beads were recovered by centrifugation for 1 min at 16 000 *g* and washed 5 times with 1 mL of cold wash buffer (Lysis buffer with 500 mM NaCl). Proteins were eluted from the beads with 30 µl of 2X laemmli buffer, heated 5 min at 95 °C, and stored at -20 °C.

Samples were separated on NuPage 4-12% Bis-Tris pre-cast gels (Invitrogen) with 1X MES buffer and antioxidant (Invitrogen) then processed for Western Blotting for OTX2 detection. Membranes were blocked in 5% non-fat milk, TBS, 0.2% Tween, incubated with anti-OTX2 (in-house mouse monoclonal) overnight at 4 °C then incubated with HRP-conjugated anti-mouse (GeneTex) for 2 h at room temperature. Chemiluminescence reaction was performed with ECL femto (Thermo Scientific).

Statistical analysis

Prism 6 software (GraphPad) was used for all statistical analysis. Sample size was determined after preliminary experiments. Quantification was normalized by the mean value of vehicle-injected mice samples. Normal data distribution was assessed by the D'Agostino & Pearson omnibus normality test. If normal test was not passed, Mann-Whitney was applied; otherwise, unpaired t-test with Welch's correction was used (noted t-test in Legends). See Figure Legends for relevant statistical tests.

Results

Otx2 knockdown in choroid plexus reduces newborn neurons in the olfactory bulb

Intracerebroventricular (icv) injections of vectorized Cre recombinase (Cre-Tat) leads to specific recombination of *Otx2* in lateral ventricle ChP of *Otx2*$^{lox/lox}$ (Otx2-lox) mice (Spatazza et al., 2013). With this paradigm, we find that Cre-Tat icv injection leads not only to a strong decrease in OTX2 protein in lateral ventricle ChP compared to vehicle-injected mice (Fig. 1*A*), but also a decrease in *Otx2* mRNA expression in the 4th ventricle ChP (41.1% ± 14.3 SD, Fig. 1*B*). These icv injections in lateral ventricles lead to a proportional decrease of *Otx2* mRNA expression in both lateral and 4th ventricle ChP (Fig. 1*C*). Therefore, the 4th ventricle ChP can be used to assess *Otx2* expression levels in ChP while anterior tissues can be used for histological quantification. Otx2-lox mice with less than 30% *Otx2* expression knockdown in the 4th ventricle after Cre-Tat icv injection where excluded from subsequent analysis.

To assess whether *Otx2* knockdown in ChP alters V-SVZ neurogenesis, we used BrdU treatments to measure either newborn neuron integration in OB (three weeks post-injection, Fig. 1*D,E*) or cell proliferation in V-SVZ (two hours post-injection, Fig. 1*J,K*) after Cre-Tat or vehicle icv injections. We found a significant decrease in granule cell layer (GCL) newborn neurons (75.6% ± 21.3 SD, Fig. 1*F*) but no change in glomerular layer (GL) newborn neurons (92.2% ± 22.8 SD, Fig. 1*G*) after *Otx2* knockdown. Analysis of caspase-expressing cells revealed no change in cell death in the RMS of Cre-Tat-injected mice (89.9% ± 31.2 SD, Fig. 1*H,I*), suggesting that OTX2 does not affect neuroblast survival. However, *Otx2* knockdown in ChP does not alter V-SVZ cell proliferation (98.6% ± 13.7 SD, Fig. 1*L*), suggesting that the observed decrease in newborn neurons is due to effects on neuroblast migration.

Non-cell-autonomous Otx2 in V-SVZ and RMS

Given that OTX2 is secreted from ChP into the CSF and accumulates in brain parenchyma (Spatazza et al., 2013), we hypothesized that OTX2 transfers from ChP to the V-SVZ niche. The *Otx2* locus is silent in V-SVZ and RMS, as shown by the absence of GFP expression in *Otx2*$^{+/GFP}$ mice (Fig. 2*A,B*) and by *in situ* hybridization (Fig. 2*C*). However, OTX2 protein is immunoprecipitated from lysates of V-SVZ and RMS microdissections (Fig. 2*D*) but not from striatum lysates (microdissection beneath V-SVZ); lysates of superior colliculus, in which *Otx2* locus is active, were used as positive control (Fig. 2*E*). Immunostaining showed selective presence of OTX2 in a subset of cells within the V-SVZ and RMS (Fig. 3), suggesting it could be targeting either neural stem cells or progenitor cells directly and/or other cells within the niche. OTX2 is not internalized in neuroblasts (DCX+ cells) in V-SVZ but accumulates in a small number of GFAP-labeled cells and many ependymal cells (Fig. 3A,*B*). In RMS, OTX2 is again absent in neuroblasts yet is in almost all GFAP labeled cells (Fig. 3*C,D*).

OTX2 protein in regions of neuroblast proliferation and migration suggests that reduced newborn neurons in OB after *Otx2* ChP knockdown in Otx2-lox mice (Fig. 1*F*) could be due in part to OTX2 non-cell-autonomous activity. To test this hypothesis, we used the scFv-Otx2 mouse model which conditionally expresses a single chain antibody (scFv) that blocks transfer by sequestering OTX2 in the CSF (Bernard et al., 2016). Cre-Tat icv injection leads to local scFv-Otx2 expression by ChP cells (GFP reporter, Fig. 4*A*) and secretion into the CSF (Bernard et al., 2016). Subjecting these mice to the BrdU paradigm for OB integration (Fig. 1*D*) revealed a decrease in newborn neurons in the GCL of Cre-Tat-injected animals (71.7% ± 17.8 SD, Fig. 4*B*) and no significant change in the GL (82.9% ± 14.7 SD, Fig. 4*B*). TUNEL assay revealed no change in neuroblast survival upon arrival in the OB (Fig. 4*C*). Taken together, these results are similar to what was observed in Otx2-lox mice (Fig. 1*F,G*) and suggests that the transfer of OTX2 transfer from CSF to V-SVZ plays a significant role in regulating adult neurogenesis. The accumulation of OTX2 protein in supporting cells (Fig. 3) within the niche further suggests that OTX2 regulates V-SVZ neurogenesis though modification of the niche microenvironment.

OTX2 regulates astrocyte factors

As we observe OTX2 internalization all along the migrating route of neuroblasts and no change in cell proliferation, we focused on a possible role for astrocytes found in both V-SVZ and RMS. Several receptors and factors are expressed in V-SVZ and RMS astrocytes that could potentially alter microenvironment composition and signaling. These include extracellular matrix (ECM) proteins such as thrombospondin (Thbs1 and Thbs4) and tenascin-C (Tnc) (Jankovski and Sotelo, 1996; Girard et al., 2014) and signaling molecules such as Robo and Eph receptors along with Ephrin ligands (Kaneko et al., 2010; Ming and Song, 2011; Falcão et al., 2012; Gengatharan et al., 2016; Todd et al., 2017), which may be under transcriptional control of OTX2 (Gherzi et al., 1997; Boncinelli and Morgan, 2001; Hoch et al., 2015; Peña et al., 2017). Expression analysis on V-SVZ microdissection lysates from the scFv-Otx2 non-cell autonomous OTX2 knock-down model showed that *EphrinA1*, *Thbs1*, *Thbs4* and *Tnc* were upregulated in V-SVZ (Fig. 5*A*). We also found that both *Thbs4* and *Tnc* were upregulated in V-SVZ of Cre-Tat injected Otx2-lox mice (304.6% ± 114.5 SD and 201.1% ± 94 SD of vehicle, respectively), reinforcing the similarity between both mice models.

To confirm that astrocytes are directly implicated in these changes in expression, we turned to an *in vitro* astrocyte model with OTX2 protein treatment. This gain-of-function paradigm resulted in the down-regulation of these same factors (Fig. 5*B*), with the exception of *Thbs4*, which is not expressed in our cultured astrocytes in-keeping with previous studies (Cahoy et al., 2008; Eroglu, 2009). In this *in vitro* paradigm, OTX2 was also found to regulate *EphrinA2* and *Eph4* expression which further highlights differences with adult V-SVZ astrocytes. While the astrocytes in this *in vitro* model do not perfectly represent isolated V-SVZ supporting cells (i.e. absence of *Thbs4* expression), they nonetheless suggest that OTX2 transfers to niche astrocytes and regulates neurogenesis by controlling ECM composition and signaling.

Discussion

OTX2 homeoprotein was previously found to act non-cell-autonomously in cortical interneurons (Sugiyama et al., 2008; Spatazza et al., 2013; Lee et al., 2017). The *Otx2* locus is not active in the V-SVZ and RMS, but the protein can be immunoprecipitated, indicating that OTX2 homeoprotein transfers not only into several distant cortical regions but also into regions proximal to the lateral ventricles. In the cortex, OTX2 is specifically internalized by parvalbumin interneurons, which have a unique and stable ECM called perineuronal nets (PNNs) that often stain for the lectin *Wisteria floribunda* (WFA) (Sugiyama et al., 2008). The specificity of internalization arises from a glycosaminoglycan-binding motif in OTX2 protein (Beurdeley et al., 2012; Lee et al., 2017), and although specific target glycosaminoglycans of OTX2 have yet to be identified, OTX2 preferentially binds di-sulfated chondroitin sulfate proteoglycans (Beurdeley et al., 2012; Miyata et al., 2012). However, staining for WFA is not detected in the V-SVZ (data not shown), which is not surprising given that PNNs are synonymous with consolidation of ECM and a break on plasticity – events that would counter the function of the neurogenic niche. The hypothesis of ECM-OTX2 interaction accounting for the specific internalization remains the most plausible, given that homeoprotein cell-surface receptors have not been found (Bernard and Prochiantz, 2016). Thus, the specificity of OTX2 for astrocytes within the V-SVZ and RMS suggests they are expressing glycosaminoglycans with high affinity for OTX2.

Through specific conditional recombination in the ChP of two mouse models, similar decreases in neurogenesis were observed. In Otx2-lox mice, recombination results in loss of local OTX2 expression in the ChP, while in scFv-Otx2 mice it results in sequestering OTX2 in

the CSF due to single chain antibody secretion by the ChP. The first model includes both potential cell-autonomous effects of loss of OTX2 in the ChP as well as potential non-cell-autonomous effects through reduced levels of secreted OTX2. The second model comprises only non-cell-autonomous effects as only secreted OTX2 is affected. This is confirmed by the absence of autocrine effects (i.e. CSF OTX2 signaling on ChP) assessed by ChP mRNA levels of OTX2 transcription targets upon scFv expression (Bernard et al., 2016). Since both models provide a similar reduction in the number of newborn neurons, it suggests that OTX2 non-cell-autonomous function is of primary importance for adult neurogenesis.

OTX2 was detected in few GFAP-positive cells in the V-SVZ, in the majority if not all of the GFAP-positive cells in the RMS, and in ependymal cells of the V-SVZ wall. While a ~20% decrease in OB newborn neurons occurred after *Otx2* knockdown, and no changes in V-SVZ proliferation nor in cell death in RMS and OB were observed, we hypothesize that OTX2 influences neuroblast migration by regulating ECM composition. Indeed, the RMS is composed of a compacted neuroblast network forming chains that migrate along blood vessels and are surrounded by astrocytic processes (Lois et al., 1996; Whitman et al., 2009). While it is clear that RMS-associated astrocytes interact with neuroblasts (Kaneko et al., 2010), the role of astrocytes for neuroblast migration is not well known. Studies show that neurogenesis is impacted by the composition of ECM in stem cells niches (Dityatev et al., 2010), which include astrocyte-derived Tnc and Thbs4 in V-SVZ and RMS (Jankovski and Sotelo, 1996; Benner et al., 2013; Girard et al., 2014), and OTX2 has been shown to regulate *Tnc* and *Thbs4* transcription (Gherzi et al., 1997; Peña et al., 2017). While *Tnc* knockout mice show no signs of altered adult neurogenesis (Kazanis et al., 2007), *Thbs4* knockout adult mice show reduced newborn neurons in the OB yet no defect of embryonic neurogenesis (Girard et al., 2014). Reduction of OTX2 in V-SVZ resulted in increased *Thbs4* expression yet decreased neurogenesis, contrary to what might be expected given the results with *Thbs4* knockout mice, suggesting complex non-binary regulation of ECM composition. Furthermore, cell-autonomous OTX2 expression was found to parallel *Thbs4* expression in the retina (Housset et al., 2013), suggesting that OTX2 activity is context dependent as previously suggested (Buecker et al., 2014). However, given the global dysregulation observed, we cannot conclude on the role of the different ECM molecules and interacting proteins. Nevertheless, changes in V-SVZ expression of *Tnc* and *Thbs4* upon *Otx2* knockdown are in-keeping with a transcriptional role for non-cell autonomous OTX2 in astrocytes.

As OTX2 was found in RMS astrocytes and that signalization with neuroblasts is still an open question (Chaker et al., 2016), we tested if genes coding for migration and signaling factors might be modified in our models. Robo2 is strongly expressed in RMS astrocytes and is required for proper RMS organization and guidance of neuroblasts (Kaneko et al., 2010), and it has been hypothesized that astrocyte-derived laminin helps form RMS scaffold for neuroblast migration (Belvindrah et al., 2007). Also, EphA4 and EphrinA2 are expressed in RMS and V-SVZ supporting astrocytes (along with other combinations of Ephs and Ephrins) and EphA4 has been shown to be critical for maintaining a compact and organized RMS (Todd et al., 2017). While OTX2 has been shown to bind Robo2 promoter (Hoch et al., 2015) and to regulate Ephrin-A2 (Rhinn et al., 1999), we did not detect any changes in V-SVZ expression after OTX2 knock-down. However, OTX2 affected expression more widely in cultured astrocytes, including expression of EphA4 and EphrinA2, suggesting it has the potential to influence RMS organization.

Non-cell autonomous OTX2 transfers from ChP to supporting astrocytes to regulate ECM molecules and factors that likely impact neuroblast migration and ultimately newborn neuron numbers. This multi-level role of OTX2 reinforces both choroid plexus and V-SVZ non-neurogenic astrocytes as key niche compartments affecting adult neurogenesis.

Acknowledgements
This work was supported by Région Ile-de-France via le DIM Cerveau et Pensée, by ERC Advanced Grant HOMEOSIGN n°339379, and by GRL Program n°2009-00424.

Author Contributions
APl, VOM, APr and AAD designed the experiments; APl, VOM and CD performed the experiments; APl, VOM and AAD wrote the manuscript.

References
Acampora D, Di Giovannantonio LG, Di Salvio M, Mancuso P, Simeone A (2009) Selective inactivation of Otx2 mRNA isoforms reveals isoform-specific requirement for visceral endoderm anteriorization and head morphogenesis and highlights cell diversity in the visceral endoderm. Mech Dev 126:882–897.

Acampora D, Omodei D, Petrosino G, Garofalo A, Savarese M, Nigro V, Di Giovannantonio LG, Mercadante V, Simeone A (2016) Loss of the Otx2-Binding Site in the Nanog Promoter Affects the Integrity of Embryonic Stem Cell Subtypes and Specification of Inner Cell Mass-Derived Epiblast. Cell Rep 15:2651–2664.

Belvindrah R, Hankel S, Walker J, Patton BL, Müller U (2007) Beta1 integrins control the formation of cell chains in the adult rostral migratory stream. Journal of Neuroscience 27:2704–2717.

Benner EJ, Luciano D, Jo R, Abdi K, Paez-Gonzalez P, Sheng H, Warner DS, Liu C, Eroglu C, Kuo CT (2013) Protective astrogenesis from the SVZ niche after injury is controlled by Notch modulator Thbs4. Nature 497:369–373.

Bernard C, Prochiantz A (2016) Otx2-PNN Interaction to Regulate Cortical Plasticity. Neural Plast 2016:1–7.

Bernard C, Vincent C, Testa D, Bertini E, Ribot J, Di Nardo AA, Volovitch M, Prochiantz A (2016) A Mouse Model for Conditional Secretion of Specific Single-Chain Antibodies Provides Genetic Evidence for Regulation of Cortical Plasticity by a Non-cell Autonomous Homeoprotein Transcription Factor. Hébert JM, ed. PLoS Genet 12:e1006035.

Beurdeley M, Spatazza J, Lee HHC, Sugiyama S, Bernard C, Di Nardo AA, Hensch TK, Prochiantz A (2012) Otx2 binding to perineuronal nets persistently regulates plasticity in the mature visual cortex. Journal of Neuroscience 32:9429–9437.

Bjornsson CS, Apostolopoulou M, Tian Y, Temple S (2015) It takes a village: constructing the neurogenic niche. Dev Cell 32:435–446.

Boncinelli E, Morgan R (2001) Downstream of Otx2, or how to get a head. Trends Genet 17:633–636.

Buecker C, Srinivasan R, Wu Z, Calo E, Acampora D, Faial T, Simeone A, Tan M, Swigut T, Wysocka J (2014) Reorganization of enhancer patterns in transition from naive to primed pluripotency. Cell Stem Cell 14:838–853.

Cahoy JD, Emery B, Kaushal A, Foo LC, Zamanian JL, Christopherson KS, Xing Y, Lubischer JL, Krieg PA, Krupenko SA, Thompson WJ, Barres BA (2008) A transcriptome database for astrocytes, neurons, and oligodendrocytes: a new resource for understanding brain development and function. Journal of Neuroscience 28:264–278.

Chaker Z, Codega P, Doetsch F (2016) A mosaic world: puzzles revealed by adult neural stem cell heterogeneity. Wiley Interdiscip Rev Dev Biol 5:640–658.

Curto GG, Nieto-Estévez V, Hurtado-Chong A, Valero J, Gómez C, Alonso JR, Weruaga E, Vicario-Abejón C (2014) Pax6 is essential for the maintenance and multi-lineage differentiation of neural stem cells, and for neuronal incorporation into the adult olfactory bulb. Stem Cells Dev 23:2813–2830.

Dityatev A, Seidenbecher CI, Schachner M (2010) Compartmentalization from the outside: the extracellular matrix and functional microdomains in the brain. Trends Neurosci 33:503–512.

Eroglu C (2009) The role of astrocyte-secreted matricellular proteins in central nervous system development and function. J Cell Commun Signal 3:167–176.

Falcão AM, Marques F, Novais A, Sousa N, Palha JA, Sousa JC (2012) The path from the choroid plexus to the subventricular zone: go with the flow! Front Cell Neurosci 6:34.

Fossat N, Chatelain G, Brun G, Lamonerie T (2006) Temporal and spatial delineation of mouse Otx2 functions by conditional self-knockout. EMBO Rep 7:824–830.

Gengatharan A, Bammann RR, Saghatelyan A (2016) The Role of Astrocytes in the Generation, Migration, and Integration of New Neurons in the Adult Olfactory Bulb. Front Neurosci 10:149.

Gherzi R, Briata P, Boncinelli E, Ponassi M, Querzè G, Viti F, Corte G, Zardi L (1997) The human homeodomain protein OTX2 binds to the human tenascin-C promoter and trans-represses its activity in transfected cells. DNA Cell Biol 16:559–567.

Girard F, Eichenberger S, Celio MR (2014) Thrombospondin 4 deficiency in mouse impairs neuronal migration in the early postnatal and adult brain. Mol Cell Neurosci 61:176–186.

Hoch RV, Lindtner S, Price JD, Rubenstein JLR (2015) OTX2 Transcription Factor Controls Regional Patterning within the Medial Ganglionic Eminence and Regional Identity of the Septum. Cell Rep 12:482–494.

Housset M, Samuel A, Ettaiche M, Bemelmans A, Béby F, Billon N, Lamonerie T (2013) Loss of otx2 in the adult retina disrupts retinal pigment epithelium function, causing photoreceptor degeneration. Journal of Neuroscience 33:9890–9904.

Jankovski A, Sotelo C (1996) Subventricular zone-olfactory bulb migratory pathway in the adult mouse: cellular composition and specificity as determined by heterochronic and heterotopic transplantation. J Comp Neurol 371:376–396.

Kaneko N, Marín O, Koike M, Hirota Y, Uchiyama Y, Wu JY, Lu Q, Tessier-Lavigne M, Alvarez-Buylla A, Okano H, Rubenstein JLR, Sawamoto K (2010) New neurons clear the

path of astrocytic processes for their rapid migration in the adult brain. Neuron 67:213–223.

Kazanis I, Belhadi A, Faissner A, Ffrench-Constant C (2007) The adult mouse subependymal zone regenerates efficiently in the absence of tenascin-C. Journal of Neuroscience 27:13991–13996.

Kokovay E, Wang Y, Kusek G, Wurster R, Lederman P, Lowry N, Shen Q, Temple S (2012) VCAM1 Is Essential to Maintain the Structure of the SVZ Niche and Acts as an Environmental Sensor to Regulate SVZ Lineage Progression. Cell Stem Cell 11:220–230.

Lee HHC, Bernard C, Ye Z, Acampora D, Simeone A, Prochiantz A, Di Nardo AA, Hensch TK (2017) Genetic Otx2 mis-localization delays critical period plasticity across brain regions. Mol Psychiatry 22:680–688.

Lehtinen MK, Bjornsson CS, Dymecki SM, Gilbertson RJ, Holtzman DM, Monuki ES (2013) The choroid plexus and cerebrospinal fluid: emerging roles in development, disease, and therapy. Journal of Neuroscience 33:17553–17559.

Lledo P-M, Valley M (2016) Adult Olfactory Bulb Neurogenesis. Cold Spring Harb Perspect Biol 8.

Lois C, García-Verdugo JM, Alvarez-Buylla A (1996) Chain migration of neuronal precursors. Science 271:978–981.

Ming G-L, Song H (2011) Adult neurogenesis in the mammalian brain: significant answers and significant questions. Neuron 70:687–702.

Mirzadeh Z, Doetsch F, Sawamoto K, Wichterle H, Alvarez-Buylla A (2010) The subventricular zone en-face: wholemount staining and ependymal flow. J Vis Exp.

Mirzadeh Z, Merkle FT, Soriano-Navarro M, Garcia-Verdugo JM, Alvarez-Buylla A (2008) Neural stem cells confer unique pinwheel architecture to the ventricular surface in neurogenic regions of the adult brain. Cell Stem Cell 3:265–278.

Miyata S, Komatsu Y, Yoshimura Y, Taya C, Kitagawa H (2012) Persistent cortical plasticity by upregulation of chondroitin 6-sulfation. Nat Neurosci 15:414–422.

Peña CJ, Kronman HG, Walker DM, Cates HM, Bagot RC, Purushothaman I, Issler O, Loh Y-HE, Leong T, Kiraly DD, Goodman E, Neve RL, Shen L, Nestler EJ (2017) Early life stress confers lifelong stress susceptibility in mice via ventral tegmental area OTX2. Science 356:1185–1188.

Petrik D, Myoga MH, Grade S, Gerkau NJ, Pusch M, Rose CR, Grothe B, Götz M (2018) Epithelial Sodium Channel Regulates Adult Neural Stem Cell Proliferation in a Flow-Dependent Manner. Cell Stem Cell 22:865–878.e868.

Prochiantz A, Di Nardo AA (2015) Homeoprotein Signaling in the Developing and Adult Nervous System. Neuron 85:911–925.

Rhinn M, Dierich A, Le Meur M, Ang S (1999) Cell autonomous and non-cell autonomous functions of Otx2 in patterning the rostral brain. Development 126:4295–4304.

Sawamoto K, Wichterle H, Gonzalez-Perez O, Cholfin JA, Yamada M, Spassky N, Murcia NS, Garcia-Verdugo JM, Marin O, Rubenstein JLR, Tessier-Lavigne M, Okano H, Alvarez-Buylla A (2006) New neurons follow the flow of cerebrospinal fluid in the adult brain. Science 311:629–632.

Shen Q, Wang Y, Kokovay E, Lin G, Chuang S-M, Goderie SK, Roysam B, Temple S (2008) Adult SVZ stem cells lie in a vascular niche: a quantitative analysis of niche cell-cell interactions. Cell Stem Cell 3:289–300.

Silva-Vargas V, Crouch EE, Doetsch F (2013) Adult neural stem cells and their niche: a dynamic duo during homeostasis, regeneration, and aging. Curr Opin Neurobiol 23:935–942.

Silva-Vargas V, Maldonado-Soto AR, Mizrak D, Codega P, Doetsch F (2016) Age-Dependent Niche Signals from the Choroid Plexus Regulate Adult Neural Stem Cells. Cell Stem Cell 19:643–652.

Spatazza J, Lee HHC, Di Nardo AA, Tibaldi L, Joliot A, Hensch TK, Prochiantz A (2013) Choroid-plexus-derived Otx2 homeoprotein constrains adult cortical plasticity. Cell Rep 3:1815–1823.

Sugiyama S, Di Nardo AA, Aizawa S, Matsuo I, Volovitch M, Prochiantz A, Hensch TK (2008) Experience-dependent transfer of Otx2 homeoprotein into the visual cortex activates postnatal plasticity. Cell 134:508–520.

Todd KL, Baker KL, Eastman MB, Kolling FW, Trausch AG, Nelson CE, Conover JC (2017) EphA4 Regulates Neuroblast and Astrocyte Organization in a Neurogenic Niche. Journal of Neuroscience 37:3331–3341.

Whitman MC, Fan W, Rela L, Rodriguez-Gil DJ, Greer CA (2009) Blood vessels form a migratory scaffold in the rostral migratory stream. J Comp Neurol 516:94–104.

Yang S-H, Kalkan T, Morissroe C, Marks H, Stunnenberg H, Smith A, Sharrocks AD (2014) Otx2 and Oct4 drive early enhancer activation during embryonic stem cell transition from naive pluripotency. Cell Rep 7:1968–1981.

Figure Legends

Figure 1. OTX2 knockdown in the choroid plexus reduces newborn neurons in the olfactory bulb. ***A-C***, Conditional *Otx2* knockdown with Otx2-lox mice. ***A***, Staining for OTX2 in lateral ventricle choroid plexus 35 d after intracerebroventricular (icv) injection of vehicle or Cre-Tat. Scale bar, 200 µm. ***B***, Quantitative PCR analysis of *Otx2* expression in 4th ventricle (****P<0.0001, Mann-Whitney test, 5 experiments). ***C***, Comparison of *Otx2* expression levels between lateral and 4th ventricles from the same brain after Cre-Tat icv injection (r=0.757, ***P<0.001, Spearman correlation, n=17). ***D***, Schematic of adult (3 months) neurogenesis study paradigm. ***E***, Staining for BrdU in olfactory bulbs 3 weeks after BrdU injections. Scale bar, 400 µm. ***F***, Quantification of BrdU-positive cells in granule cell layer (GCL) (***P<0.001, t-test, 3 experiments). ***G***, Quantification of BrdU-positive cells in glomerular layer (GL) (*ns*=P>0.05, t-test, 3 experiments). ***H***, Staining for caspase and DCX in RMS. Scale bar, 100 µm. (**i**) Quantification of caspase/DCX co-labeled cells in RMS (*ns*=P>0.05, Mann-Whitney test, 3 experiments). ***J***, Schematic of adult (3 months) V-SVZ proliferation study paradigm. ***K***, Staining for BrdU in V-SVZ 2 hours after BrdU injection. Scale bar, 200 µm. ***L***, Quantification of BrdU-positive cells in V-SVZ (*ns*=P>0.05, t-test, 2 experiments). Error bars represent SD.

Figure 2. OTX2 in RMS and V-SVZ is non-cell-autonomous**.** ***A-C***, Absence of *Otx2* expression in V-SVZ (***A, C***) and RMS (***B***) as shown by GFP staining in coronal sections of *Otx2*$^{+/GFP}$ mice (***A, B***) and by *in situ* hybridization for *Otx2* mRNA in coronal sections of wild-type mice (***C***). Note the expression of GFP in choroid plexus (***A***) and of *Otx2* in septum (***C***). Scale bars, 100 µm (***A, B***), 250 µm (***C***). ***D***, Representative sagittal section of RMS microdissection. Scale bar, 1 mm. ***E,*** Western blot analysis of OTX2 immunoprecipitation from lysates of various brain regions. Bands include OTX2 (<40 kDa), IgG (25 and 55 kDa), and unknown (~45 kDa). SC, superior colliculus; Str, striatum (n=3 for each brain region).

Figure 3. OTX2 transfers into supporting cells of neurogenic niches. ***A***, In dorsal V-SVZ, OTX2 staining is detected in some GFAP-labeled astrocytes but not in DCX-labeled neuroblasts. Scale bar, 100 µm. Arrows highlight astrocytes containing OTX2. ***B***, Along the lateral ventricular wall, OTX2 staining is detected in vimentin (Vim) labeled ependymal cells. Scale bar, 30 µm. ***C***, In the RMS, OTX2 staining is detected in GFAP-labeled astrocytes but not in DCX-labeled neuroblasts. Scale bar, 30 µm. Arrows highlight astrocytes containing OTX2. ***D***, Orthogonal projection shows OTX2 in the nucleus of astrocytes within the RMS.

Figure 4. Non-cell autonomous OTX2 is sufficient to regulate adult neurogenesis. ***A***, Efficient recombination in choroid plexus of scFv-Otx2 mice after icv injection of Cre-Tat assessed by GFP reporter. Scale bar, 200 µm. ***B***, Quantification of BrdU-positive cells in granule cell layer (GCL) and glomerular layer (GL) to assess adult neurogenesis (paradigm in Fig. 1*D*) in scFv-Otx2 mice (*ns*=P>0.05, **P< 0.01, t-test, 3 experiments). ***C***, TUNEL analysis of GCL and GL to assess cell death in scFv-Otx2 mice (*ns*=P>0.05, t-test, 2 experiments). Error bars represent SD.

Figure 5. OTX2 regulates expression of ECM and signaling proteins. ***A***, Quantitative PCR analysis of V-SVZ expression in scFv-Otx2 after icv injection of Cre-Tat or vehicle (*ns*=P>0.05, *P<0.05, **P<0.01, Mann-Whitney test, n=5 to 7). ***B***, Quantitative PCR analysis of OTX2-treated astrocyte cultures (**P<0.01, ****P< 0.0001, Mann-Whitney test, n=8 to 12). Error bars represent SD.

Figure 1

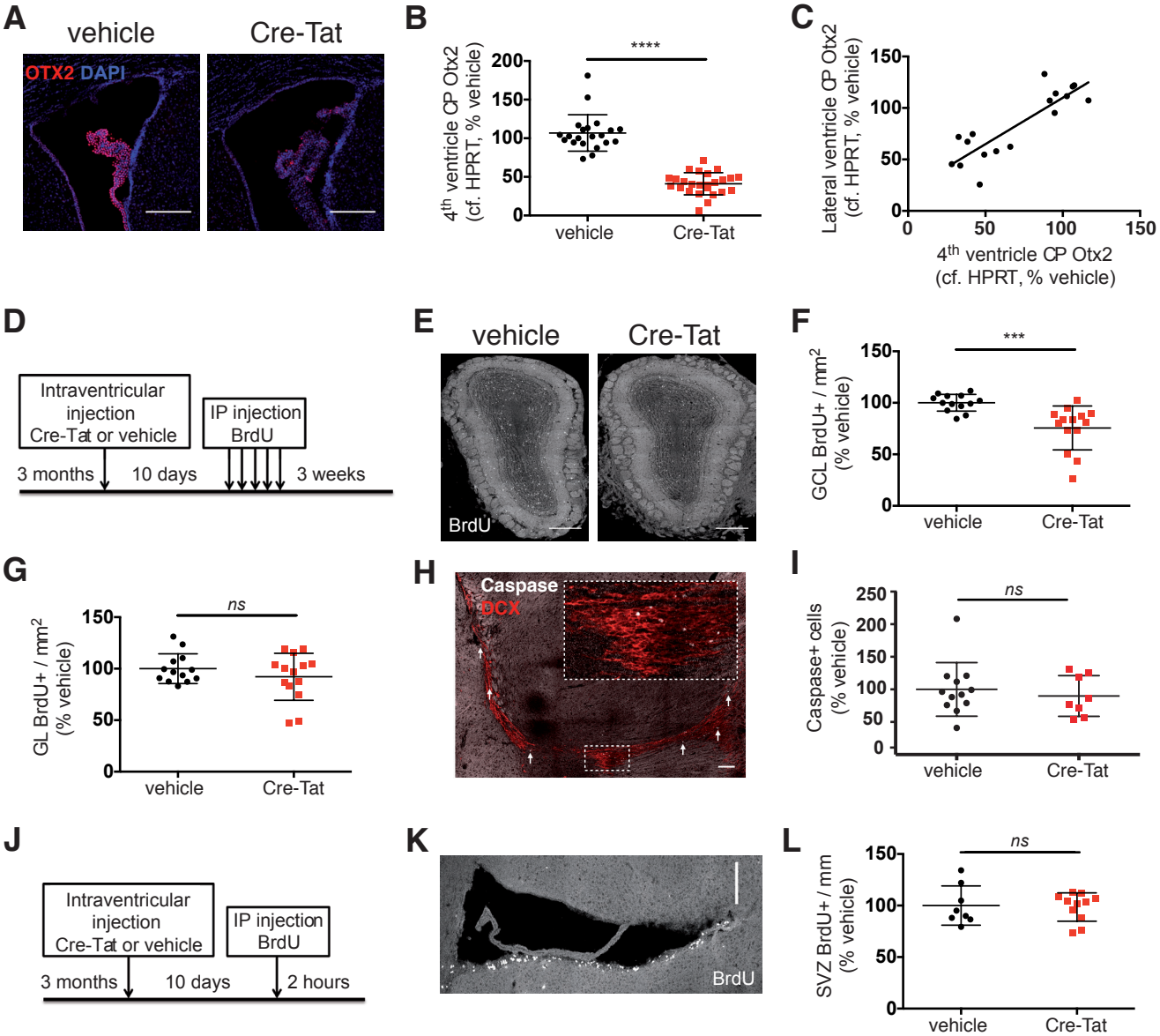
A
vehicle
Cre-Tat
OTX2 DAPI
B
4th ventricle CP Otx2 (cf. HPRT, % vehicle)
****
vehicle
Cre-Tat
C
Lateral ventricle CP Otx2 (cf. HPRT, % vehicle)
4th ventricle CP Otx2 (cf. HPRT, % vehicle)
D
Intraventricular injection Cre-Tat or vehicle
IP injection BrdU
3 months
10 days
3 weeks
E
vehicle
Cre-Tat
BrdU
F
GCL BrdU+ / mm2 (% vehicle)
***
vehicle
Cre-Tat
G
GL BrdU+ / mm2 (% vehicle)
ns
vehicle
Cre-Tat
H
Caspase
DCX
I
Caspase+ cells (% vehicle)
ns
vehicle
Cre-Tat
J
Intraventricular injection Cre-Tat or vehicle
IP injection BrdU
3 months
10 days
2 hours
K
BrdU
L
SVZ BrdU+ / mm (% vehicle)
ns
vehicle
Cre-Tat

Figure 2

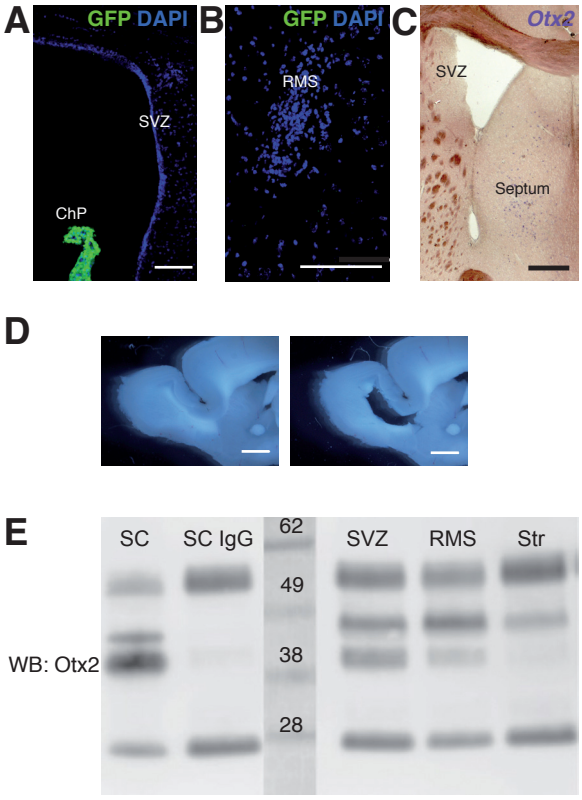
A
GFP DAPI
SVZ
ChP
B
GFP DAPI
RMS
C
Otx2
SVZ
Septum
D
E
SC
SC IgG
62
49
38
28
SVZ
RMS
Str
WB: Otx2

Figure 3

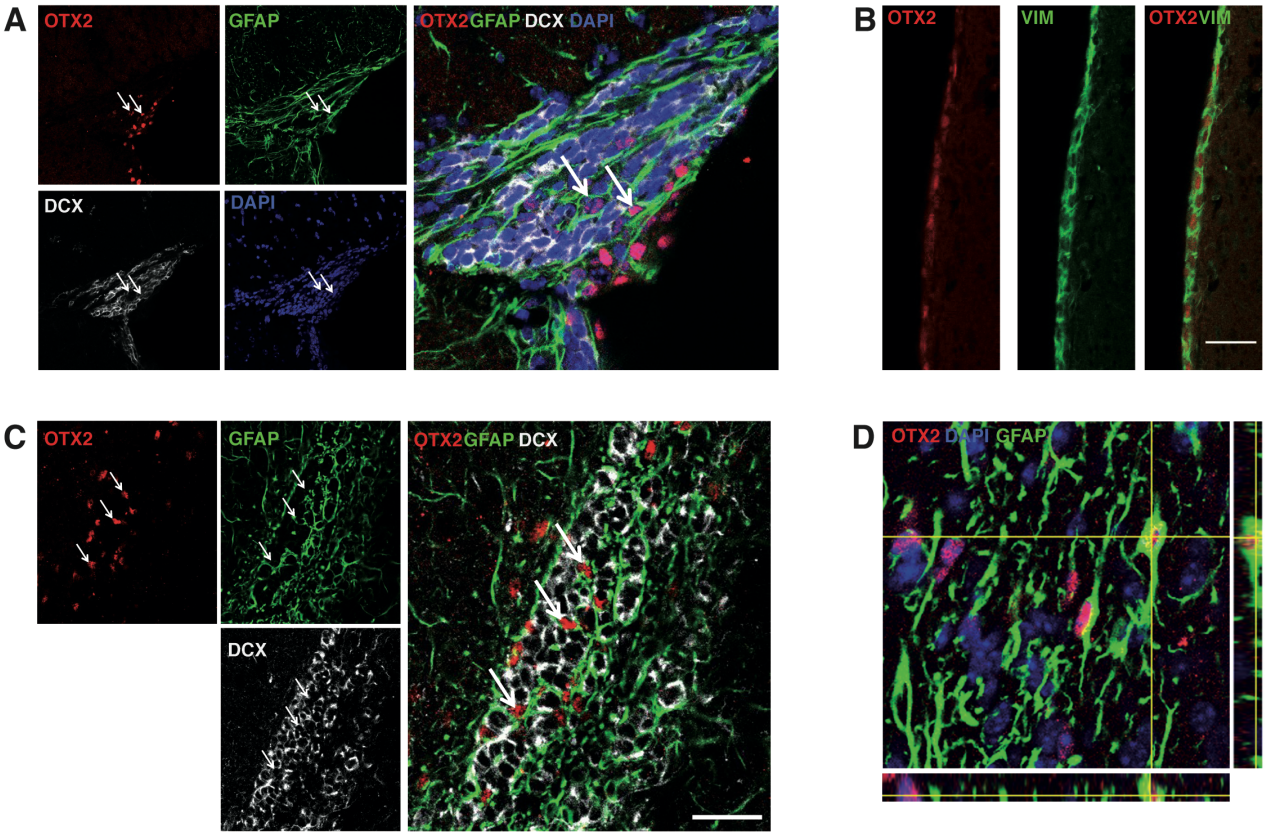
A
OTX2
GFAP
OTX2 GFAP DCX DAPI
DCX
DAPI
B
OTX2
VIM
OTX2 VIM
C
OTX2
GFAP
OTX2 GFAP DCX
DCX
D
OTX2 DAPI GFAP

Figure 4

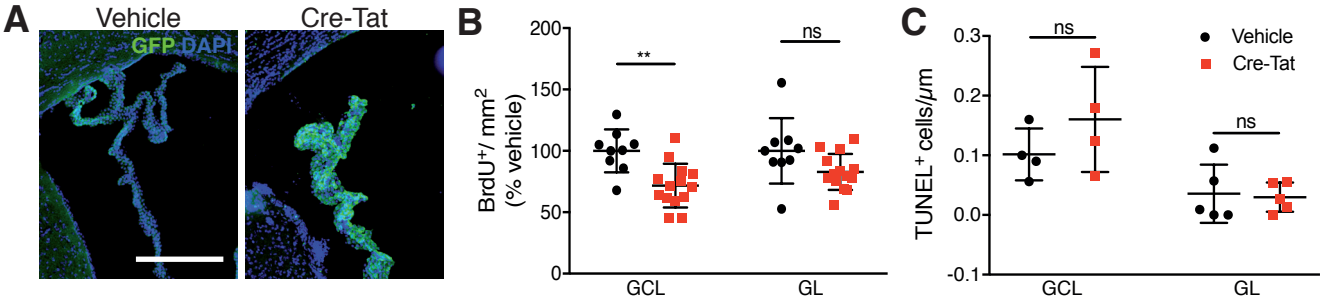
A
Vehicle
Cre-Tat
GFP DAPI
B
BrdU+/ mm2 (% vehicle)
200
150
100
50
0
**
ns
GCL
GL
C
TUNEL+ cells/µm
0.3
0.2
0.1
0.0
-0.1
ns
ns
Vehicle
Cre-Tat
GCL
GL

Figure 5

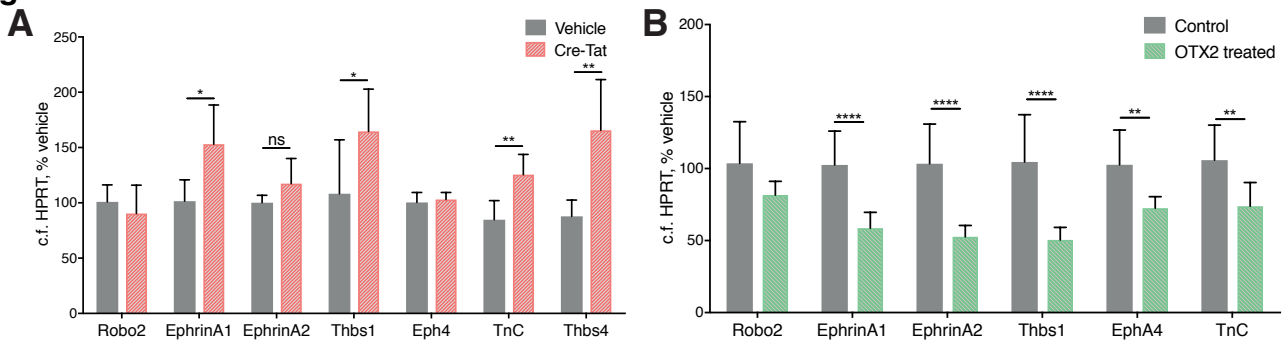
A
Vehicle
Cre-Tat
c.f. HPRT, % vehicle
250
200
150
100
50
0
*
ns
*
**
**
Robo2
EphrinA1
EphrinA2
Thbs1
Eph4
TnC
Thbs4
B
Control
OTX2 treated
c.f. HPRT, % vehicle
200
150
100
50
0
****
****
****
**
**
Robo2
EphrinA1
EphrinA2
Thbs1
EphA4
TnC